JOURNAL OF VIROLOGY, Nov. 2007, p. 11604–11611 Vol. 81, No. 21
0022-538X/07/$08.00+0 doi:10.1128/JVI.01130-07

Identification of Acetylated, Tetrahalogenated Benzimidazole D-Ribonucleosides with Enhanced Activity against Human Cytomegalovirus▽

Jae-Seon Hwang,[1] Oliver Kregler,[1] Rita Schilf,[1] Norbert Bannert,[2] John C. Drach,[3,4] Leroy B. Townsend,[4] and Elke Bogner[1]*

Institut für Virologie, Charité Universitätsmedizin Berlin, Berlin, Germany[1]; Robert Koch-Institut, Berlin, Germany[2]; and Department of Biologic and Materials Sciences, School of Dentistry,[3] and Interdepartmental Graduate Program in Medicinal Chemistry, College of Pharmacy,[4] University of Michigan, Ann Arbor, Michigan

Received 24 May 2007/Accepted 18 July 2007

DNA packaging is the key step in viral maturation and involves binding and cleavage of viral DNA containing specific DNA-packaging motifs. This process is mediated by a group of specific enzymes called terminases. We previously demonstrated that the human cytomegalovirus (HCMV) terminase is composed of the large subunit pUL56 and the small subunit pUL89. While the large subunit mediates sequence-specific DNA binding and ATP hydrolysis, pUL89 is required only for duplex nicking. An excellent inhibitor targeting HCMV terminase is 2-bromo-5,6-dichloro-1-(β-D-ribofuranosyl)benzimidazole (BDCRB), but it was not developed as an antiviral drug due to its metabolic cleavage in experimental animals. We now have tested several new benzimidazole D-ribonucleosides in order to determine whether these compounds represent new, potent inhibitors. Analysis by bioluminometric ATPase activity assays identified two of the new compounds with a high inhibitory effect, 2-bromo-4,5,6-trichloro-1-(2,3,5-tri-*O*-acetyl-β-D-ribofuranosyl) benzimidazole (BTCRB) and 2,4,5,6-tetrachloro-1-(2,3,5-tri-*O*-acetyl-β-D-ribofuranosyl benzimidazole (Cl_4RB). By using viral plaque formation, viral yield, and viral growth kinetics, we demonstrated that the two compounds BTCRB and Cl_4RB had antiviral activities similar to that of BDCRB. Interestingly, BTCRB retained its inhibitory activity after preincubation with HFF cells. By use of electron microscopy, we observed an increase of B capsids and a lack of cytoplasmic capsids in the presence of the compounds that correlated with the virus yield. Furthermore, cleavage of concatenated DNA was inhibited by both compounds, and inhibition by BTCRB was shown to be dose dependent. These results demonstrate that the new compounds are highly active against HCMV and act by mechanisms similar but not identical to those of BDCRB.

Human cytomegalovirus (HCMV) is a member of the herpesvirus family and represents a major human pathogen, causing severe disease in newborns and immunocompromised patients, i.e., organ transplant recipients and patients with AIDS. HCMV is classified as a betaherpesvirus and is characterized by its narrow host range and prolonged replicative cycle in permissive cells (10, 26). Maturational events of HCMV DNA replication and capsid assembly require cleavage of concatenated DNA into genome length, followed by insertion into preformed capsids. The following six steps are involved in this process: (i) The recognition of viral DNA by a specific protein able to (ii) bind the DNA at specific sequence motifs (packaging signals, e.g., pac1 and pac2), (iii) translocation of the DNA-protein complex to the procapsid, (iv) interaction of the DNA-protein complex with the portal protein, (v) import of one unit-length genome into the capsid, involving ATP hydrolysis by one terminase subunit, and (vi) completion of the packaging process by cleavage of excess DNA (two-strand nicking). Several gene products of HCMV have been identified that appear to be involved in the process of DNA replication, cleavage, and packaging (13, 15).

Enzymes involved in the viral DNA packaging process are responsible for site-specific duplex nicking and insertion of the DNA into the procapsids (2, 11). These enzymes are known as terminases and power the packaging via their ATPase activity. More recently, we have demonstrated that the HCMV terminase is composed of two subunits, the large one encoding pUL56 and the small one pUL89 (5–6), where each protein has a different function. While the large subunit mediates sequence-specific DNA binding and ATP hydrolysis, pUL89 is required only for duplex nicking (19, 28–29). Furthermore, together with the portal protein the terminase form a nanomotor that enables the translocation of the DNA into the capsid. In the case of Phi 29, it has been demonstrated that the force of the packaging motor is as much as 57 pN, thus representing one of the strongest biological nanomotors (18, 31). Unlike ATP-hydrolyzing terminase subunits of most other icosahedral virions, e.g., double-stranded-DNA bacteriophages and herpes simplex virus type 1, the large subunit pUL56 is stably associated with the capsid and represents a structural component (1, 3, 30, 36). Only one other terminase protein, P9 of bacteriophage PRD1, is also a structural component of the virion (25, 33). Recently we presented the first three-dimensional structural data for pUL56 and showed by single-particle electron microscopy in conjunction with digital image analysis that pUL56 forms a dimer with a C-2 symmetry (27).

The benzimidazole D-ribonucleosides 2,5,6-trichloro-1-(β-D-ribofuranosyl)benzimidazole (TCRB) and 2-bromo-5,6-dichloro-1-(β-D-ribofuranosyl)benzimidazole (BDCRB) are po-

* Corresponding author. Mailing address: Institut für Virologie, Charité Campus Mitte, Charitéplatz 1, 10117 Berlin, Germany. Phone: 49-30-450525121. Fax: 49-30-450525907. E-mail: elke.bogner@charite.de.

▽ Published ahead of print on 29 August 2007.

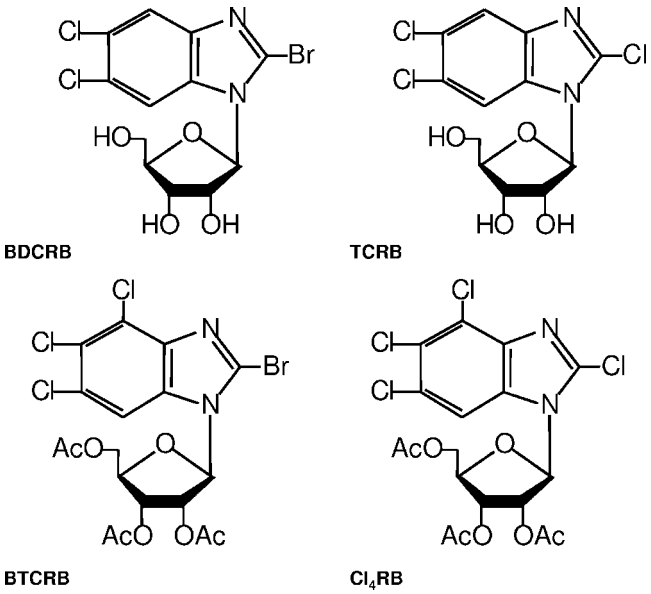

FIG. 1. Structures of benzimidazole D-ribonucleosides BDCRB, TCRB, Cl_4RB, and BTCRB.

tent and selective inhibitors of HCMV replication (34). HCMV strains resistant to these compounds were selected and had resistance mutations in pUL89 (35) or pUL89 and pUL56 (21–22). Interestingly, we subsequently demonstrated that the specific HCMV terminase inhibitor BDCRB inhibited pUL56-specific ATPase activity (27, 29). In this study, we identified new benzimidazole analogs that prevent the ATPase activity of pUL56 and one analog that is more stable.

MATERIALS AND METHODS

Cells and viruses. 5B1-4 (High five) insect cells were grown in TC-100 medium supplemented with 10% fetal calf serum (FCS), glutamine, and gentamicin (60 μg/ml). For generation of recombinant baculovirus, transposition into the bacmid bMON14272 was used as described by Luckow et al. (24).

Human foreskin fibroblasts (HFF) were grown in Dulbecco's minimal essential medium (DMEM) supplemented with 10% FCS, 2 mM glutamine, penicillin (5 U/ml), and streptomycin (50 μg/ml). HFF cells at passages 10 to 15 were used for infections, and experiments were carried out with confluent cell monolayers (1.5×10^7 cells). Preparation of HCMV AD169 was performed after infection of HFF cells at a multiplicity of infection (MOI) of 0.1.

Immunofluorescence. For immunofluorescence, HFF cells were grown on coverslips. At the appropriate time point, cells were fixed with 3% paraformaldehyde as described previously (32). After staining, the samples were mounted in Fluoroprep (bioMerieux) with 2.5% (wt/vol) 1,4-diazabicyclo[2.2.2]octan and examined by immunofluorescence microscopy using an Olympus BX 50. Images were captured with an Olympus Colorview II camera in conjunction with Cell D software (Olympus Soft Imaging Solutions; kindly donated by Sonnenfeld-Foundation, Berlin, Germany).

Benzimidazole nucleosides. BDCRB, TCRB, 2,4,5,6-tetrachloro-1-(2,3,5-tri-*O*-acetyl-β-D-ribofuranosyl)benzimidazole (Cl_4RB), 2-bromo-4,5,6-trichloro-1-(2,3,5-tri-*O*-acetyl-β-D-ribofuranosyl)benzimidazole (BTCRB), and the deacetylated homologs of Cl_4RB and BTCRB were synthesized in the laboratory of L. B. Townsend (Fig. 1).

Bioluminometric ATPase assay. Purified rpUL56 (0.3 μg), extracts from insect cells (High five), or apyrase (EC 3.6.1.5) was incubated in 200 μl of ATPase buffer (100 mM Tris-acetate, pH 7.5, 2 mM EDTA, 10 mM magnesium acetate, 0.1% bovine serum albumin, 1 mM dithiothreitol) containing 20 μg D-luciferin and 1 ng luciferase. The samples were incubated at 30°C for 30 min prior to initiation of the reaction by injection of 40 μl of a 0.2-pmol ATP stock solution. Luminescence was measured with a microplate luminometer (OrionII; Berthold Detection Systems). By using the software Simplicity, the measurement parameters were defined (fast kinetics; measurement time, 40 s). The results were displayed in real time on the screen and the data exported directly into the Excel software program. This assay allows a direct measurement of the ATP hydrolysis of the proteins by the amount of decreasing ATP.

Plaque reduction assay. Human foreskin fibroblasts were seeded in a 24-well plates and infected with HCMV AD169 with a MOI of 0.01 in DMEM with 10% FCS. After 1 h postinfection (p.i.), the inoculum was replaced by 2 ml methyl cellulose (Methocel MC; Fluka) containing DMEM, 3% FCS, and inhibitors. All inhibitors were used in dilutions in duplicate. After incubation for 8 days at 37°C, the cells were stained with 0.1% crystal violet (in 20% ethyl alcohol) for 2 min and air dried prior to rinsing in Aqua dest. Plaques were counted by using a microscope. Drug effects were calculated by comparing drug-treated cells to untreated cells.

Cytotoxicity determination. Cytotoxicity profiling of the benzimidazole D-ribonucleosides was determined by the use of a Cell Proliferation Kit II (XTT) (Roche) as recommended by the manufacturer.

Yield assay. HFF (4×10^4 cells) were seeded in 96-well plates and infected with HCMV AD169 with a MOI of 1 in the absence or presence of BDCRB, BTCRB, or Cl_4RB. By serial dilution, concentrations of 0.1 μM to 100 μM were tested. After 7 days p.i., the supernatants were subjected to one cycle of freezing and thawing prior to transfer of a 100-μl aliquot to a new 96-well monolayer culture of HFF cells. After serial 1:3 dilution across the plate, the cells were incubated for an additional 7 days. The cells were fixed and stained with crystal violet as described above. Plaques were enumerated by microscopic counting.

Stability assay. HFF cells (25-cm^2 flask; 2×10^6 cells) were incubated with 10 μM BDCRB, BTCRB, and Cl_4RB or without an inhibitor. After 48 h, the preincubated supernatants were transferred to a new 12-well plate infected with HCMV AD169 at a MOI of 0.01. The concentrations tested were 1.0 and 0.2 μM. After 7 days of incubation, the cells were fixed and stained with crystal violet and the plaques were counted by using a microscope as described before.

Growth characteristics. HFF cells (1×10^5 cells per well) were seeded in 24-well culture plates. Confluent cells were infected with AD169 at a MOI of 1 in the absence or presence of 10 μM BTCRB, Cl_4RB, or BDCRB. At 24, 48, 72, and 96 h p.i., the supernatants were harvested and frozen at −80°C. After collection at all time points, the supernatant were thawed and transferred to a 12-well plate, and titers were determined by plaque reduction assay as described above.

Expression and purification of recombinant protein. Insect cells (5B1-4 [High five, 4×10^8]) expressing the recombinant protein (rpUL56) (6) were harvested 48 h p.i. Sedimented cells were lysed in 50 ml cation exchange buffer (20 mM morpholineethanesulfonic acid [pH 6.5], 150 mM NaCl, and complete protease inhibitor cocktail [Roche Applied Science]) and sonicated on ice. Cell lysates were sedimented and passed through a 0.2-μm filter prior to loading onto an equilibrated cation exchange column (HiTrap SP HP, 1-ml bed volume; Amersham Bioscience). The purification was performed at 4°C by using an ÄKTA-prime (Amersham Bioscience) chromatograph. Elution was achieved using a linear salt gradient from 50 mM to 2 M NaCl in 20 mM morpholineethanesulfonic acid (pH 6.5). Fractions containing the protein were subjected to the second purification step with gel filtration carried out with a HiLoad 16/60 Superdex 200 prep grade gel permeation column using an ÄKTA fast-performance liquid chromatography system (Amersham Bioscience) as described previously (28).

Pulsed-field gel electrophoresis (PFGE). HFF cells (2×10^6 cells per well) were seeded in a 25-cm^2 flask, infected at an MOI of 1, and treated without or with 1 nM, 10 nM, 100 nM, 1 μM, 10 μM, or 30 μM BTCRB or with 30 μM Cl_4RB for 5 days. Cells were scraped, resuspended in 150 μl L buffer (100 mM EDTA, 10 mM Tris-HCl [pH 7.5], 20 mM NaCl), and mixed with 150 μl 2% SeaPlaque GTG agarose (Bio-Rad) and 10 mg/ml proteinase K prior to embedding in blocks. Lysation was performed by incubation of the agarose block in 10 ml lysis buffer (100 mM EDTA, 10 mM Tris-HCl [pH 7.5], 20 mM NaCl, 1% sarcosyl sodium, 100 μg/ml proteinase K) at 50°C overnight. Proteinase K was inactivated in 10 volumes of TE buffer (10 mM Tris-HCl, 10 mM EDTA [pH 8.0]) and 1 mM phenylmethylsulfonyl fluoride for 48 h at room temperature. Agarose blocks were equilibrated in 0.5× Tris-borate-EDTA buffer for 30 min. The blocks were loaded into the pockets of a 1% agarose gel, and parameters were as follows: 20-h run at 14°C, 120° pulse angle, voltage gradient of 6 V/cm, and pulse time of 5 s with a linear ramp to 30 s. DNA was stained with 1 μg/ml ethidium bromide for 60 min and photographed. The image was inverted by using Adobe Photoshop CS software. By using an HCMV green fluorescent protein (GFP) bacterial artificial chromosome (BAC) (7–8), the size of the monomers was determined to be 230 kb.

Thin sectioning and electron microscopy. HFF cells (25-cm^2 flask, 1×10^6 cells) were infected with HCMV AD169 at a MOI of 1 in the presence and absence of 35 μM BTCRB, Cl_4RB, or BDCRB. Cells were fixed with 20 mM

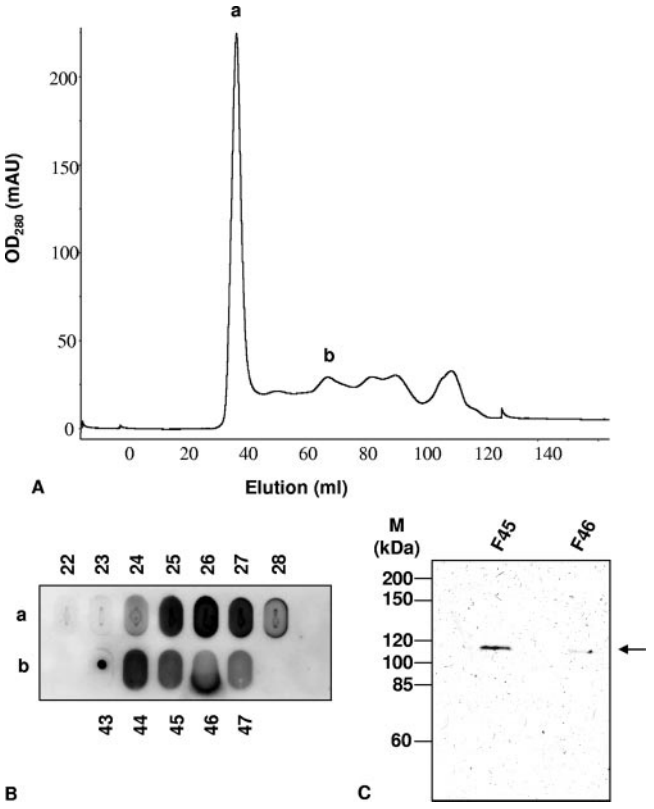

FIG. 2. Purification of recombinant expressed pUL56. (A) Gel permeation chromatography of rpUL56. Single-step-purified rpUL56 was subjected to chromatography through a HiLoad 16/60 SuperdexTM 200 prep column using an ÄKTAExplorer with results recorded by OD_{280}. (B) The peak fractions (a and b) were subjected to dot blot analysis. (C) Fractions 45 and 46 were separated on a sodium dodecyl sulfate gel prior to immunoblot analysis with pAbUL56. Molecular mass markers are indicated on the left side, the position of rpUL56 on the right side.

HEPES (pH 7.4) containing 2.5% glutaraldehyde, 4% paraformaldehyde, and 1% tannin for 90 min at room temperature, dehydrated, poststained with 1% osmium tetroxide and 0.2% (wt/vol) uranyl acetate, and subsequently embedded in glycid ether 100 (Carl Roth) with 1.5% (wt/vol) 1-methyl-5-norbornene-2,3-dicarboxylic acid anhydride, methylnadic anhydride (Carl Roth). Polymerization was performed at 60°C for 3 days prior to sectioning with Ultracut S (Reichert-Jung). The sections were transferred to slot grids coated with Pioloform (Plano, Wetzlar, Germany) and stained for 10 min with 1% (wt/vol) uranyl acetate in 40% ethyl alcohol followed by lead citrate staining for an additional 10 min (9). The sections were analyzed by using a FEI Technai electron microscope operated at 120 kV.

RESULTS

Purification of rpUL56. The protein pUL56 was expressed as a recombinant baculovirus and purified by two chromatographic steps, including cation exchange and gel permeation chromatography. Aliquots of the rpUL56-containing fractions after gel permeation chromatography (Fig. 2A) were assayed for protein content by dot blot analysis on nitrocellulose. The nitrocellulose filters were reacted with affinity-purified antibodies against pUL56 (pAbUL56) (16). Fractions 24 to 28 (corresponding to 34 to 40 ml elution volume) and 44 to 47 (corresponding to 65 to 70 ml elution volume) containing rpUL56 (Fig. 2B) were used for further analysis. The purity of fractions 44 and 45 was demonstrated by sodium dodecyl sulfate-polyacrylamide gel electrophoresis prior to Coomassie staining (Fig. 2C).

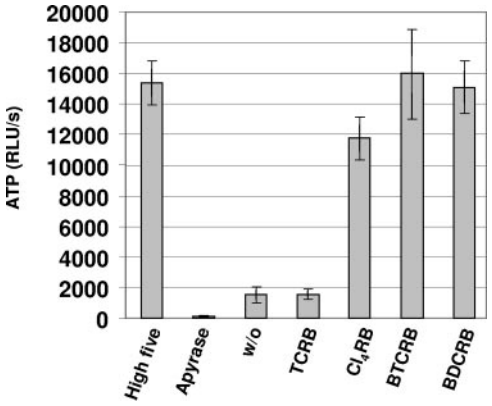

FIG. 3. Bioluminometric ATPase activity assay. Extracts from High five cells (High five), apyrase, or purified pUL56 without (w/o) or in the presence of 100 μM TCRB, dBDCRB, CDMRB, Cl_4RB, BTCRB, or BDCRB were preincubated in the assay mixture for 30 min at 30°C prior to when the reaction was started by addition of ATP. The degradation of ATP was detected by the luciferase system. Error bars on the histogram are standard deviations for five independent experiments.

Activity of new benzimidazole D-ribonucleosides. In order to determine if a compound had an inhibitory effect, the capacity to block the ATPase activity of the large terminase subunit pUL56 was analyzed by bioluminometric ATPase activity assays. The purified recombinant protein rpUL56 (fraction 45) (Fig. 2) was incubated in the presence of different compounds for 30 min at 30°C prior to addition of ATP for starting the reaction.

The fraction containing the purified rpUL56 showed a decrease in the ATP concentration (Fig. 3). Extracts from insect cells were used as a negative control and apyrase (EC 3.6.1.5.) as a positive control (Fig. 3). While the enzymatic activity of rpUL56 in the presence of 100 μM BDCRB and BTCRB was completely inhibited, Cl_4RB reduced the activity by approximately fivefold while TCRB had no effect (Fig. 3), thus demonstrating that BDCRB and BTCRB are the most efficient inhibitors of pUL56 enzymatic activity.

Analysis of antiviral activity in infected cells. After selection of compounds, their antiviral activity was quantified by four methods: (i) measurement of viral plaque formation (plaque reduction assay), (ii) measurement of growth kinetics, (iii) analysis of the stability in vivo, and (iv) measurement of released particles by electron microscopy (thin sectioning). For determination of the 50% infective concentration (IC_{50}), plaque reduction assays were performed. The mean IC_{50}s were 0.50 ± 0.18 μM for BTCRB and 0.25 ± 0.19 μM for Cl_4RB, compared to 0.49 ± 0.29 μM for BDCRB (Table 1). All compounds were active against HCMV in plaque as well as yield assays (90% infective concentration [IC_{90}]) but were not cytotoxic at concentrations lower than 30 μM (Table 1). According to our recent finding that only Cl_4RB inhibits the interaction of pUL56 with pUL104, the observation of similar antiviral activities of the different analogs is no indication of the same modes of action (12).

TABLE 1. Antiviral activities of benzimidazole D-ribonucleosides

Compound	Mean IC_{50} (μM) for plaque reduction	Mean IC_{90} (μM) for yield assay	Mean CC_{50} (μM) for cell proliferation[a]
BDCRB	0.49 ± 0.29	0.29	313.6 ± 17.21
Cl_4RB	0.25 ± 0.19	0.27	66.7 ± 2.57
BTCRB	0.50 ± 0.18	0.20	27.8 ± 2.02

[a] CC_{50}, 50% cytotoxicity.

Single-cycle growth curves were measured with cells infected in the absence or presence of 10 μM BTCRB, Cl_4RB, or BDCRB in order to determine the effect on replication. As shown in Fig. 4, there was a significant difference in yield and kinetics of infectious virus production. Taken together, the data presented show that the compounds possessed potent in vitro viral growth inhibition properties.

In order to determine whether the new compounds are more stable in vivo than BDCRB, the compounds were preincubated with HFF cells for 48 h. The supernatants were transferred to HFF cells infected with AD169. In the presence of 1.0 μM of BTCRB and Cl_4RB, plaque formation was completely blocked, compared to a slight reduction of approximately 11% in the case of BDCRB (Fig. 5). Furthermore, even in the presence of 0.2 μM BTCRB, only 20% plaques were observed, while with 0.2 μM Cl_4RB, more than 70% plaques were formed in comparison with the control (Fig. 5). This effect was not seen with BDCRB at the concentrations tested (Fig. 5). These data clearly demonstrated that BTCRB has excellent stability in cell culture, thus representing a promising new compound.

In addition, the activities of the deacetylated homologs of Cl_4RB and BTCRB were evaluated in plaque and yield reduction assays. Their activities (IC_{50} for plaque reduction = 0.3 and 0.23 μM; IC_{90} for yield = 0.01 and 0.18 μM, respectively) were similar to those of the acetylated compounds (Table 1),

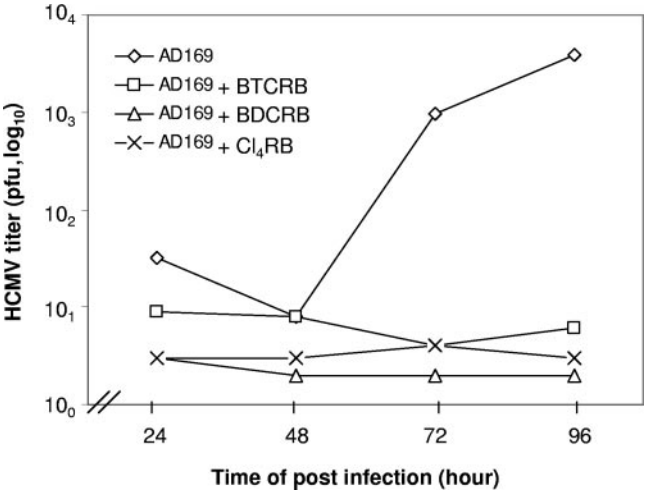

FIG. 4. Growth kinetics in the presence of BTCRB. HFF cells were infected with HCMV AD169 at a MOI of 1 in the absence or presence of 10 μM BTCRB. At each time point, cells and supernatants were harvested and progeny virus titers were determined by plaque reduction assay.

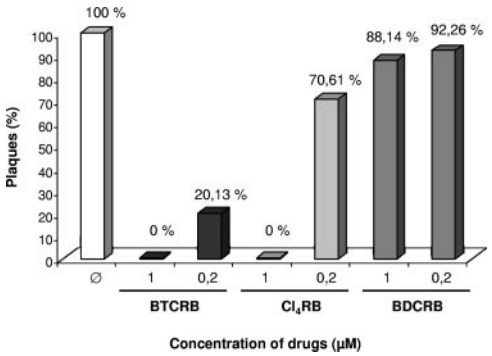

FIG. 5. Stability of the compounds in vivo. After 48 h of preincubation of 1.0 or 0.2 μM Cl_4RB, BTCRB, or BDCRB with HFF cells, the supernatants were incubated for an additional 7 days on infected HFF cells (MOI of 0.01). The resulting plaques were counted after crystal violet staining.

suggesting that the O-acetyl compounds were most likely deacetylated in culture media and were active in the form of the ribosyl homologs.

To analyze the formation of particles, ultrathin sections of HFF cells infected with HCMV AD169 in the absence or presence of 5 μM BTCRB, Cl_4RB, or BDCRB were examined by electron microscopy. In infected cells grown without the compound, all types of capsids (B, C, and A capsids) were formed and viral particles were released (Fig. 6; Table 2). In contrast, cells infected in the presence of BTCRB, Cl_4RB, or BDCRB mainly produced B capsids and a drastically reduced number of C capsids and released only dense bodies, leading to the presumption that viral DNA packaging did not occur (Fig. 6; Table 2). Furthermore, detailed study of primary maturation at the nuclear envelope revealed aberrant budding. Several immature capsids (capsidless particles) were found in the perinuclear cisternae in cells infected in the presence of BTCRB (Fig. 7B), whereas without the compound just one capsid was determined (Fig. 7A). These experiments demonstrated that the compound BTCRB prevents DNA packaging and therefore only pro- or B capsids could be detected.

Influence of new compounds on cleavage of concatenated DNA. To analyze the structure of viral DNA which accumulated in infected cells in the presence of 10 μM BTCRB or Cl_4RB, intracellular DNA was separated by PFGE and stained with ethidium bromide. PFGE can be used to distinguish concatenated and cleaved unit-length genomes. In untreated infected cells, the viral DNA is cleaved into unit-length DNA (Fig. 8, lanes 2 and 4), while in the presence of the compounds (Fig. 8, lanes 3 and 5), most of the viral DNA remained in the pockets of the pulsed-field gel, resembling concatemers. In more detail, the inhibition of the formation of unit-length genomes is dependent on the dose of BTCRB (Fig. 9). These results indicate that both new compounds, BTCRB and Cl_4RB, have an effect on cleavage of concatemeric DNA.

DISCUSSION

Treatment of HCMV infections is still an enormous problem, because currently available drugs cause serious problems,

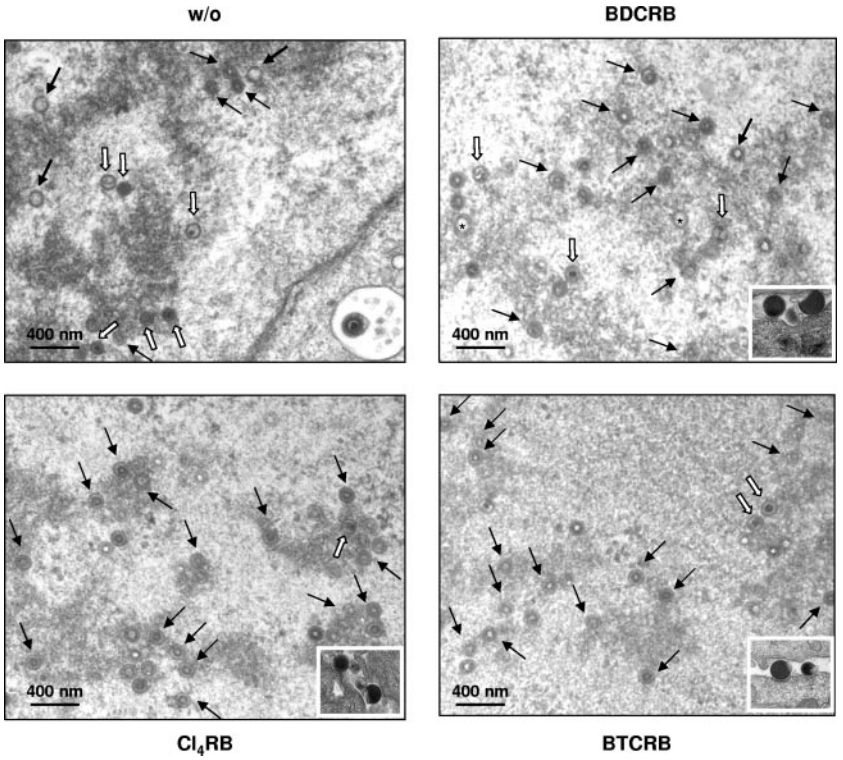

FIG. 6. Transmission electron micrographs of thin sections. HFF cells were infected with AD169 at an MOI of 1 in the absence or presence of 5 μM BTCRB, Cl_4RB, or BTCRB and analyzed by electron microscopy at 72 h p.i. B capsids are indicated by black arrows, A capsids by bold black arrows, C capsids by white arrows, and virions by white arrows. Dense bodies are shown in the integrated small figure.

such as nephrotoxicity, and have several disadvantages, such as low or no oral bioavailability. In addition, current treatment has resulted in the rising appearance of drug-resistant viral strains; thus, new targets with a different mode of action are urgently needed for immunocompromised patients. The development of benzimidazole ribonucleosides was a key step in obtaining new potent and selective antiviral compounds (34). The most prominent compound of this work is BDCRB. However, even though it is an excellent inhibitor of HCMV infection in cell culture, it is not metabolically stable in vivo. To overcome this problem, various derivates has been synthesized. In this study, we analyzed some of these analogs concerning their mode of action.

Resistance to BDCRB has been mapped to the HCMV open reading frames UL56 and UL89 (21, 35). Both proteins represent subunits of the HCMV terminase. While the large subunit, pUL56, mediates sequence-specific DNA binding, capsid association, and ATP hydrolysis, pUL89 is mainly required for cleavage of concatemers via duplex nicking (19, 28–29). Recently we demonstrated by using a new bioluminometric assay that the ATPase activity of pUL56 is completely inhibited in the presence of BDCRB (27). The established assay was used to screen selected BDCRB derivates. Interestingly, the two most effective new compounds were BTCRB and Cl_4RB. Surprisingly, TCRB had no effect on the enzymatic activity of pUL56. This is also surprising because it was TCRB, not BDCRB, which was used to isolate the drug-resistant virus that had the mutation in UL56 (21). The benzimidazole nucleosides BTCRB and Cl_4RB have identical structures except for position 2, where BTCRB possesses a bromide and Cl_4RB possesses a chloride (Fig. 1). Thus, the pUL56 ATP binding site tolerates few changes.

TABLE 2. Nuclear capsids of infected cells in absence or presence of 5 μM benzimidazole D-ribonucleosides

Virus and treatment	No. of nuclei counted	% of capsid form per nucleus		
		A	B	C
AD169	10	15.6	37.9	46.5
AD169 + BTCRB	13	14.9	70.7	14.4
AD169 + Cl_4RB	11	6.5	62.7	30.8
AD169 + BDCRB	9	10.5	61.2	28.3

Nonetheless, we tested BDCRB together with BTCRB and Cl_4RB concerning their ability to inhibit viral replication. All compounds inhibited plaque formation of AD169-infected cells (Table 1). Cl_4RB, compared to BDCRB, was the most efficient compound in these assays; however, the IC_{50}s differed only slightly (Table 1), while BTCRB has antiviral activity similar to that of BDCRB (Table 1). These results indicate that all compounds are effective against HCMV maturation.

In order to analyze the effect of the compounds on viral replication, growth curve kinetics were determined. As expected, the compounds led to a nearly complete reduction in viral yield (Fig. 4). To verify whether these compounds have an advantage for further use in therapy, we tested the stability in vivo. Interestingly, while both acetyl esters were

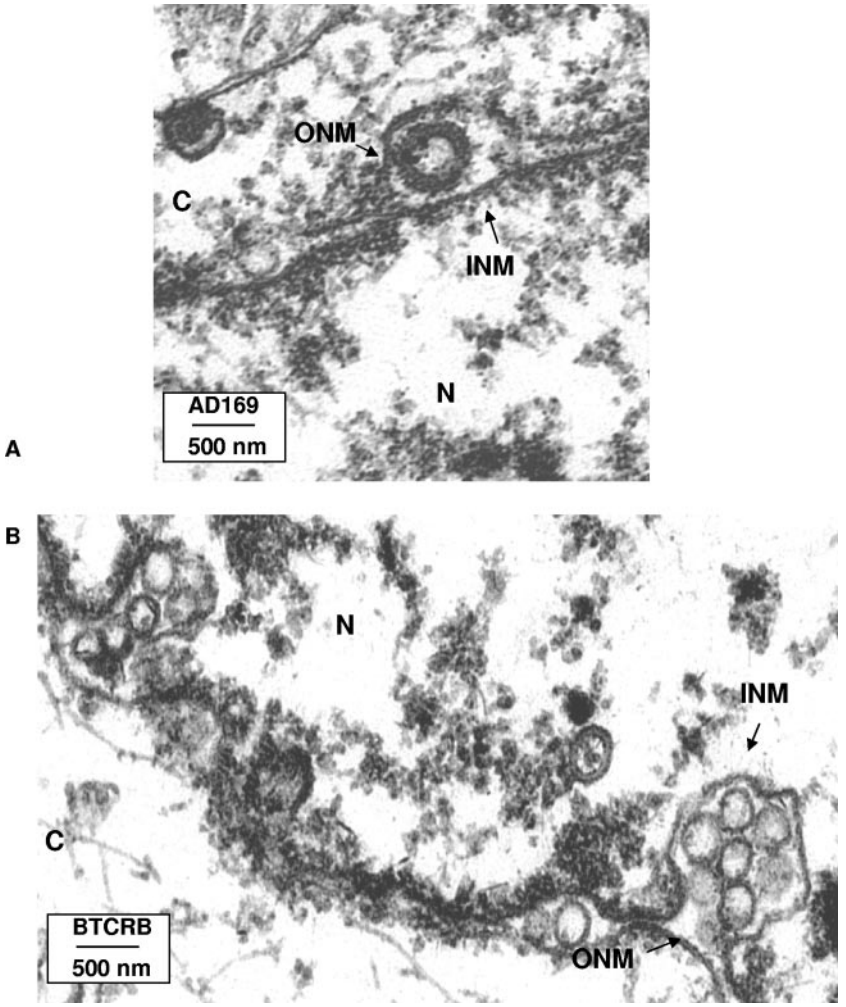

FIG. 7. Electron microscopy analysis of budding events at the nuclear membranes. (A) Enveloped particles in the perinuclear cisternae of HCMV-infected cells. (B) Capsidless particles in the perinuclear cisternae. INM, inner nuclear membrane; ONM, outer nuclear membrane; N, nucleus; C, cytoplasm.

more stable in vivo at a concentration of about 1 μM than BDCRB, BTCRB is also stable at low concentrations (Fig. 5). Since it has been shown that BDCRB is metabolized too rapidly (17), it is important to analyze the new compound BTCRB in detail.

Electron microscopy analysis demonstrated that packaging was blocked, because most capsids lack DNA, and that a block in egress through the nuclear envelope exists. Since DNA packaging requires a great amount of energy, it is reasonable that BTCRB leads to inhibition of packaging by inhibition of the pUL56 ATPase activity. The observed aberrant budding at the nuclear envelope could not be explained by the block of ATP hydrolysis. We demonstrated that Cl_4RB leads to a similar block in DNA packaging; however, the mechanism is thought to be the inhibition of the interaction of pUL56 with the portal protein (12). In addition, by pulse-field analysis we confirmed both compounds could inhibit cleavage of viral concatemers, and in the case of BTCRB, an amount of more than 100 nM is sufficient for the inhibition of cleavage. Thus, in the final analysis, the two new acetyl esters of the tetrahalogenated benzimidazoles inhibit viral DNA packaging, but the question arises as to what the primary effect of BTCRB and Cl_4RB is. If the block of cleavage into unit-length genomes were the primary function, it would result in an increase of C capsids. However, in our analysis a decreasing number of C capsids were observed in the presence of the compounds (Fig. 7). In addition, the explanation is in contrast to the block of the pUL56-associated ATPase activity that is a prerequisite for packaging, including an aberrant one. There are at least two more reasonable explanations: (i) the conformation of the protein changed in the presence of the compounds, or (ii) it is a sterical hindering that prevents viral DNA binding as well as protein-protein interaction (e.g., with the portal protein). Therefore, cleavage into unit-length genomes and packaging into the capsids would be the consequence of this primary function. It is necessary to await the development of further methods to confirm these hypotheses.

Furthermore, in the presence of BTCRB, the capsids in the nuclear cisternae resemble spherical procapsids instead of B capsids. Therefore, one could suggest that this phenomenon is

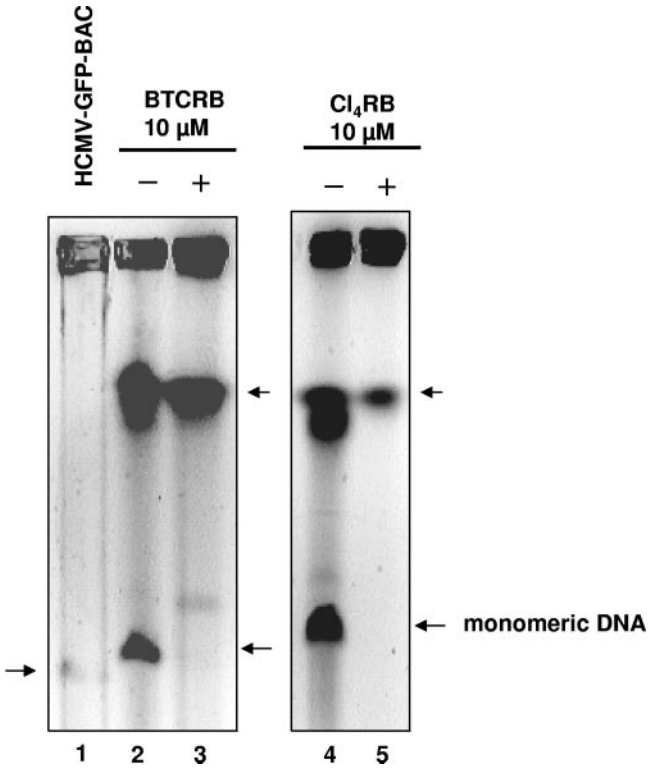

FIG. 8. Influence of the compounds on DNA cleavage and de novo synthesis. PFGE analysis of infected cells in the presence of 10 μM BTCRB and Cl_4RB. HFF cells were infected with a MOI of 1 in the absence (w/o) or presence of 10 μM BTCRB or Cl_4RB. One hundred twenty hours p.i., cells were embedded in agarose and digested with proteinase K. DNA was resolved by PFGE, stained with ethidium bromide, and photographed. Unit-length monomers are indicated. An HCMV GFP BAC was used for determination of the size.

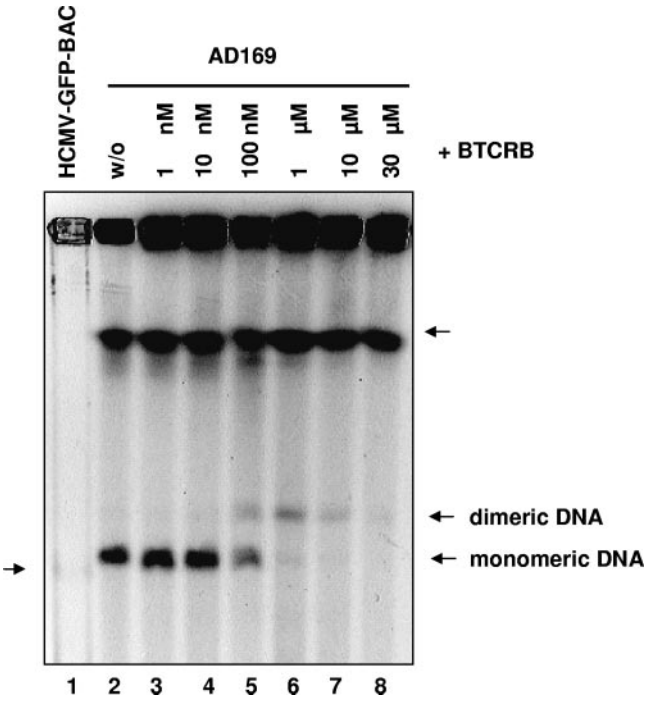

FIG. 9. PFGE analysis of infected cells in the presence of BTCRB. HFF cells were infected with a MOI of 1 in the absence (w/o) or presence of 1 nM, 10 nM, 100 nM, 1 μM, 10 μM, or 30 μM BTCRB. One hundred twenty hours p.i., cells were embedded in agarose and digested with proteinase K. DNA was resolved by PFGE, stained with ethidium bromide, and photographed. Unit-length monomers are indicated. An HCMV GFP BAC was used for determination of the size.

due to a different effect of BTCRB. Krosky et al. (23) reported that the analog of BDCRB, 1263W94 or maribavir, did block nuclear egress of C capsids. This compound, however, did not target the HCMV terminase but the UL97 protein kinase (4), as well as UL27 (20). Recently Evers et al. (14) reported that the α-5′-deoxylyxofuranosyl analog of TCRB has a distinct biochemical mode of action. This compound inhibited HCMV replication before viral DNA synthesis. These findings demonstrated that analogs of the benzimidazole ribonucleosides with different sugar moieties in some cases had distinct modes of action.

In conclusion, we identified two new tetrahalogenated acetate esters that have high antiviral activities. In the case of BTCRB, the efficient block of the ATPase activity of the large terminase subunit pUL56 leads to the formation of empty capsids and an accumulation of capsids in the perinuclear cisternae. In addition, BTCRB appears to be stable in cell culture, thus representing a promising lead for the development of future antiviral therapy. Experiments are ongoing to investigate the stability in patient sera. To verify whether BTCRB represents an attractive compound for therapy, more-extensive preclinical studies are required.

ACKNOWLEDGMENTS

This work was supported by the Wilhelm Sander Foundation (no. 2004.031.2) and by the DFG (Deutsche Forschungsgemeinschaft; BO 1214/5-4).

We are grateful to G. Holland (Robert Koch-Institut, Berlin) for performing the sectioning. We thank B. Gentry for performing the BDCRB metabolism experiment. E.B. thanks D. Krüger for kind support. O. Kregler is a recipient of a fellowship from the Sonnenfeld-Foundation Berlin.

ADDENDUM IN PROOF

Experiments completed after acceptance of the manuscript established that BDCRB was not metabolized in uninfected human foreskin fibroblasts. Analysis by HPLC of the media from cell cultures incubated with 10 or 100 μM of BDCRB for up to 48 h showed no loss or degradation of BDCRB. Thus, the results presented in Fig. 5 cannot be due to metabolism of BDCRB by preincubation with uninfected cells.

REFERENCES

1. **Beard, P. M., C. Duffy, and J. D. Baines.** 2004. Quantification of the DNA cleavage and packaging proteins UL15 and UL28 in A and B capsids of herpes simplex virus type 1. J. Virol. **78:**1367–1374.
2. **Black, L.** 1989. DNA packaging in dsDNA bacteriophages. Annu. Rev. Microbiol. **43:**267–292.
3. **Black, L. W.** 1988. DNA packaging in dsDNA bacteriophages, p. 321–373. *In* R. Calendar. (ed.), The bacteriophages. Plenum, New York, NY.
4. **Biron, K. K., R. J. Harvey, S. C. Chamberlain, S. S. Good, A. A. Smith III, M. G. Davis, C. L. Talarico, W. H. Miller, R. Ferris, R. E. Dornsife, S. C. Stanat, J. C. Drach, L. B. Townsend, and G. W. Koszalka.** 2002. Potent and selective inhibition of human cytomegalovirus replication by 1263W94, a benzimidazole L-riboside with a unique mode of action. Antimicrob. Agents Chemother. **46:**2365–2372.
5. **Bogner, E.** 2002. Human cytomegalovirus terminase as a target for antiviral chemotherapy. Rev. Med. Virol. **12:**115–127.

6. **Bogner, E., K. Radsak, and M. F. Stinski.** 1998. The gene product of human cytomegalovirus open reading frame UL56 binds the pac motif and has specific nuclease activity. J. Virol. **72:**2259–2264.
7. **Borst, E. M., G. Hahn, U. H. Koszinowski, and M. Messerle.** 1999. Cloning of the human cytomegalovirus (HCMV) genome as an infectious bacterial artificial chromosome in *Escherichia coli*: a new approach for construction of HCMV mutants. J. Virol. **73:**8320–8329.
8. **Borst, E. M., and M. Messerle.** 2000. Development of a cytomegalovirus vector for somatic gene therapy. Bone Marrow Transplant. **25:**80–82.
9. **Bozzola, J. J., and L. D. Russel.** 1998. Electron microscopy. Principles and techniques for biologists, 2nd ed. Jones and Bartlett Publishers, Boston, MA.
10. **Britt, W. J., and C. A. Alford.** 1996. Cytomegalovirus, p. 2493–2523. *In* B. N. Fields, D. M. Knipe, and P. M. Howley (ed.), Fields virology, 3rd ed. Lippincott-Raven Publishers, Philadelphia, PA.
11. **Casjens, S., and W. M. Huang.** 1982. Initiation of sequential packaging of bacteriophage P22 DNA. J. Mol. Biol. **157:**287–298.
12. **Dittmer, A., J. C. Drach, L. B. Townsend, A. Fischer, and E. Bogner.** 2005. Interaction of the putative HCMV portal protein pUL104 with the large terminase subunit pUL56 and its inhibition by benzimidazole-D-ribonucleosides. J. Virol. **79:**14660–14667.
13. **Dunn, W., C. Cou, H. Li, D. Patterson, V. Stolc, H. Zhu, and F. Liu.** 2003. Functional profiling of a human cytomegalovirus genome. Proc. Natl. Acad. Sci. USA **100:**14223–14228.
14. **Evers, D. L., G. Komazin, R. G. Ptak, D. Shin, B. T. Emmer, L. B. Townsend, and J. C. Drach.** 2004. Inhibition of human cytomegalovirus replication by benzimidazole nucleosides involves three distinct mechanisms. Antimicrob. Agents Chemother. **48:**3918–3927.
15. **Gibson, W.** 1996. Structure and assembly of the virion. Intervirology **39:**389–400.
16. **Giesen, K., K. Radsak, and E. Bogner.** 2000. The potential terminase subunit pUL56 of HCMV is translocated into the nucleus by its own NLS and interacts with importin α. J. Gen. Virol. **81:**2231–2244.
17. **Good, S. S., B. S. Owens, L. B. Townsend, and J. C. Drach.** 1994. The disposition in rats and monkey of 2-bromo-5,6-dichloro-1-(β-D-ribofuranosyl)-benzimidazole (BDCRB) and its 2,5,6-trichloro-1(β-D-ribofuranosyl)-benzimidazole (TCRB). Antiviral Res. **23**(Suppl. I)**:**103.
18. **Guo, P., and T. J. Lee.** 2007. Viral nanomotors for packaging of dsDNA and dsRNA. Mol. Microbiol. **64:**886–903.
19. **Hwang, J.-S., and E. Bogner.** 2002. ATPase activity of the terminase subunit pUL56 of human cytomegalovirus. J. Biol. Chem. **27:**6943–6948.
20. **Komazin, G., R. G. Ptak, B. T. Emmer, L. B. Townsend, and J. C. Drach.** 2003. Resistance of human cytomegalovirus to the benzimidazole L-ribonucleoside maribavir maps to UL27. J. Virol. **77:**11499–11506.
21. **Krosky, P. M., M. R. Underwood, S. R. Turk, K. W.-H. Feng, R. K. Jain, R. G. Ptak, A. C. Westerman, K. K. Biron, L. B. Townsend, and J. C. Drach.** 1998. Resistance of human cytomegalovirus to benzimidazole ribonucleosides maps to two open reading frames: UL89 and UL56. J. Virol. **72:**4721–4728.
22. **Krosky, P. M., K. Z. Borysko, M. R. Nassari, R. V. Devivar, R. G. Ptak, M. G. Davis, K. K. Biron, L. B. Townsend, and J. C. Drach.** 2002. Phosphorylation of β-D-ribosylbenzimidazoles is not required for activity against human cytomegalovirus. Antimicrob. Agents Chemother. **46:**478–486.
23. **Krosky, P. M., C. Baek, and D. M. Coen.** 2003. The human cytomegalovirus UL97 protein kinase, an antiviral drug target, is required at the stage of nuclear egress. J. Virol. **77:**905–914.
24. **Luckow, V. A., S. C. Lee, G. F. Barry, and P. O. Olins.** 1993. Efficient generation of infectious recombinant baculoviruses by site-specific transposon-mediated insertion of foreign genes into a baculovirus genome propagated in *Escherichia coli*. J. Virol. **67:**4566–4579.
25. **Mindich, L., D. Bamford, T. McGaw, and G. MacKenzie.** 1982. Assembly of bacteriophage PRD1: particle formation with wild-type and mutant viruses. J. Virol. **44:**1021–1030.
26. **Mocarski, E. S.** 1996. Cytomegaloviruses and their replication, p. 2447–2492. *In* B. N. Fields, D. M. Knipe, and P. M. Howley (ed.), Fields virology, 3rd ed. Lippincott-Raven Publishers, Philadelphia, PA.
27. **Savva, C. G. W., A. Holzenburg, and E. Bogner.** 2004. Insights into the structure of human cytomegalovirus large terminase subunit pUL56. FEBS Lett. **563:**135–140.
28. **Scheffczik, H., C. G. W. Savva, A. Holzenburg, L. Kolesnikova, and E. Bogner.** 2002. The terminase subunits pUL56 and pUL89 of human cytomegalovirus are DNA-metabolizing proteins with toroidal structure. Nucleic Acids Res. **30:**1695–1703.
29. **Scholz, B., S. Rechter, J. C. Drach, L. B. Townsend, and E. Bogner.** 2003. Identification of the ATP-binding site in the terminase subunit pUL56 of human cytomegalovirus. Nucleic Acids Res. **31:**1426–1433.
30. **Sheaffer, A. K., W. W. Newcomb, M. Gao, D. Yu, S. K. Weller, J. C. Brown, and D. J. Tenney.** 2001. Herpes simplex virus DNA cleavage and packaging proteins associate with the procapsid prior to its maturation. J. Virol. **75:**687–698.
31. **Smith, D. E., S. J. Tans, S. B. Smith, S. Grimes, D. L. Anderson, and C. Bustamante.** 2001. The bacteriophage straight phi29 portal motor can package DNA against a large internal force. Nature **413:**748–752.
32. **Smuda, C., E. Bogner, and K. Radsak.** 1997. The human cytomegalovirus glycoprotein B gene (ORF UL55) is expressed early in the infectious cycle. J. Gen. Virol. **78:**1981–1992.
33. **Strömsten, N. J., D. Bamford, and J. K. H. Bamford.** 2003. The unique vertex of bacterial virus PRD1 is connected to the viral internal membrane. J. Virol. **77:**6314–6321.
34. **Townsend, L. B., R. V. Devivar, S. R. Turk, M. R. Nassari, and J. C. Drach.** 1995. Design, synthesis, and antiviral activity of certain 2,5,6-tri-halo-1-(β-dribofuranosyl)benzimidazoles. J. Med. Chem. **38:**4098–4105.
35. **Underwood, M. R., R. J. Harvey, S. C. Stanat, M. L. Hemphill, T. Miller, J. C. Drach, L. B. Townsend, and K. K. Biron.** 1998. Inhibition of human cytomegalovirus DNA maturation by a benzimidazole ribonucleoside is mediated through the UL89 gene product. J. Virol. **72:**717–725.
36. **Yu, D., and S. K. Weller.** 1998. Herpes simplex virus type 1 cleavage and packaging proteins UL15 and UL28 are associated with B but not C capsids during packaging. J. Virol. **72:**7428–7439.